ISSN 2278-3091
Volume 9, No.1, January – February 2020
International Journal of Advanced Trends in Computer Science and Engineering
Available Online at http://www.warse.org/IJATCSE/static/pdf/file/ijatcse18912020.pdf
https://doi.org/10.30534/ijatcse/2020/18912020

Simplified Geometric Model for Generic Projector Application in Digital Fringe Profilometry

Cong Kai Yee, Kin Sam Yen
School of Mechanical Engineering, Engineering Campus, Universiti Sains Malaysia,
Nibong Tebal, Penang 14300, Malaysia.
meyks@usm.my

ABSTRACT

This research proposes a simplified geometric model for a generic projector application in digital fringe profilometry. Reported works have high number of model parameters and project at slanted angles. This increases complexity of the calibration processes and causes . The arrangement also complicates the determination of model parameters as the inner details of a projector are not revealed to end user. The proposed model enables simpler calibration by determining only three parameters, eliminating inconsistency of fringe width, and applying a more suitable light path configuration for any generic projector available off-the-shelf. Three conditions must be met for the model to function appropriately, which includes (1) the camera optical axis and projector reference line must be orthogonal to the reference plane, (2) the measured object must be within the overlapped light path area between the camera and projector, and (3) the end of the image acquisition area must be placed before the reference line of the projector. Experimental result shows that the model is capable of reconstructing object with errors recorded at 0.07 ± 0.04 mm, 0.10 ± 0.04 mm and 2.63 ± 0.20 mm for flat, slanted and curved surfaces, respectively.

Keywords: profilometry, projector, camera, 3D reconstruction, triangulation, geometric model.

1 INTRODUCTION

Digital fringe profilometry (DFP) is a non-contact, whole-field optical surface profiling technique [1,2]. It has the ability to measure millions of points simultaneously using high resolution cameras [2], enabling dynamic changes of a surface to be measured with the DFP technique. This is a great advantage, as conventional methods, such as coordinate measuring machine and laser scanning, could only measure one point at a time.

The DFP technique consists of four main components [3], namely a projector, a reference plane, a camera and a computer. A digital fringe image would be created in the computer and projected onto the object surface as a spatial marker. The projected fringe image would be distorted according to the object shape when the camera acquires it. The phase maps of the acquired fringe image on the object and ideal fringe image on the reference plane would be obtained by phase demodulation and phase unwrapping. Finally, the difference between the phase maps would then be converted into height map by triangulation. Triangulation is the process of calculating the surface height of every pixel of the fringe image based on the phase map differences and the geometrical relationship between the camera, object, projector and reference plane [3]. The configuration of the main components will affect the accuracy and ease of use of a DFP system [3].

In 1983, Takeda and Mutoh proposed a simple triangulation model[4] that strictly required the following conditions: (1) the optical centres for both camera and projector must be located at the same distance from the reference plane, (2) the plane formed by both optical axes must be perpendicular to the reference plane, and (3) the optical axis of camera must be orthogonal to the reference plane. Measurement errors were bound to occur given the practical difficulty of meeting these conditions. Therefore, a modified model was proposed which essentially allowed both optical centres to be located at different distances from the reference plane [5]. This improved model was more flexible than the model proposed by Takeda and Mutoh. Nonetheless, conditions (2) and (3) still needed to be fulfilled. In 2012, a different model was proposed which eliminated the need for locating both camera and projector optical centres at the same distance from the reference plane while also ensuring the camera optical axis were perpendicular to the reference plane [6]. In 2014, Huang et al. proposed a model that was free from the all three conditions [3]. The placement of components and configuration of the reported models are shown in Figure 1. The comparison between the aforementioned models in terms of the mathematical relationship and restrictions are listed in Table 1.

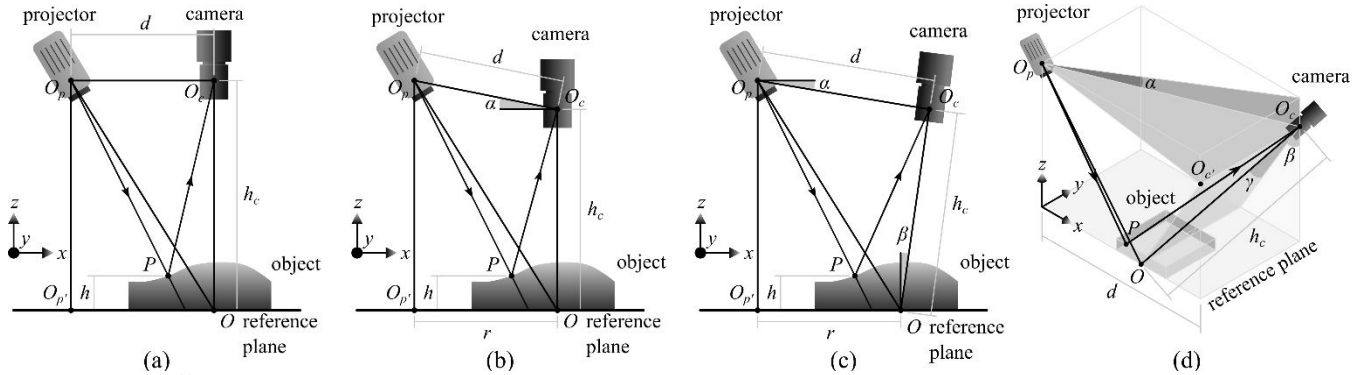

Figure 1: Different triangulation models: (a) Takeda and Mutoh [4], (b) Mao et al. [5], (c) Xiao et al. [6], and (d) Huang et al. [3].

Notwithstanding, the number of model affiliated parameters also increased from three, in Takeda and Mutoh's model, to seven, in model proposed by Huang et al. The increased number of parameters increase the number of steps and difficulty of the calibration processes. Besides that, in these models, the projector was placed in a way that allowed its optical axis to form an acute angle with a line orthogonal to the reference plane, as shown in Figure 1. This would result in an inconsistent fringe width across the whole fringe image, as shown in Figure 2 (a). Furthermore, the projected image of a projector is not symmetry around the projector optical axis, as shown in Figure 2 (b). The optical axis of a conventional projector would generally be slanted at an angle. However, the dimensions and details on the configuration of lens inside the projector were not revealed to the end user. A reference line, as shown in Figure 2 (b), is usually provided (instead of the optical axis) to calculate the ratio between projection distance and size and aspect ratio of the projection image. This would increase the difficulty in obtaining the parameters accurately without carrying out reverse engineering on the projector structure.

This research proposed a simple triangulation model to eliminate the inconsistency of fringe width while also reducing the total number of parameters needed for the phase to height conversion. The proposed model aimed its applicability to any generic projector available off-the-shelf. The working principle of the model will be discussed in more detailed in Section 2. This model is expected to reduce the complexity of the calibration process and increases measurement accuracy.

Table 1: Phase to height conversion formula and comparison between triangulation models

Models	Formula	Number of Parameters	Required Conditions
Takeda and Mutoh[4]	$h(x,y) = \frac{-h_c \cdot \Delta\varphi(x,y)}{2\pi f_0 d - \Delta\varphi(x,y)}$	3	1,2 and 3
Mao et al.[5]	$h(x,y) = \frac{-h_c(h_c + d\sin\alpha)\cdot\Delta\varphi(x,y)}{2\pi f_0 h_c r - h_c\cdot\Delta\varphi(x,y) - d\sin\alpha\cdot\varphi_P(x,y)}$	5	2 and 3
Xiao et al.[6]	$h(x,y) = \frac{-h_c(h_c\cos\beta + d\sin\alpha)\cdot\Delta\varphi(x,y)}{2\pi f_0 h_c(r\cos\beta + d\sin\alpha\sin\beta) - h_c\cos\beta\cdot\Delta\varphi(x,y) - d\sin\alpha\cdot\varphi_P(x,y)}$	6	2
Huang et al.[3]	$h(x,y) = \frac{-h_c\cos\beta\cos\gamma(h_c\cos\beta\cos\gamma + d\sin\alpha)\cdot\Delta\varphi(x,y)}{2\pi f_0 h_c(r\cos\gamma + d\sin\alpha\sin\beta) - h_c\cos\beta\cos\gamma\cdot\Delta\varphi(x,y) - d\sin\alpha\cdot\varphi_P(x,y)}$	7	-

where
f_0 is the fringe width on reference plane.
h_c is the camera optical centre height.
d is the distance between camera optical centre and projector optical centre.
$\Delta\varphi$ is the phase differences between reference plane and object surface.
φ_P is the phases on object surface.

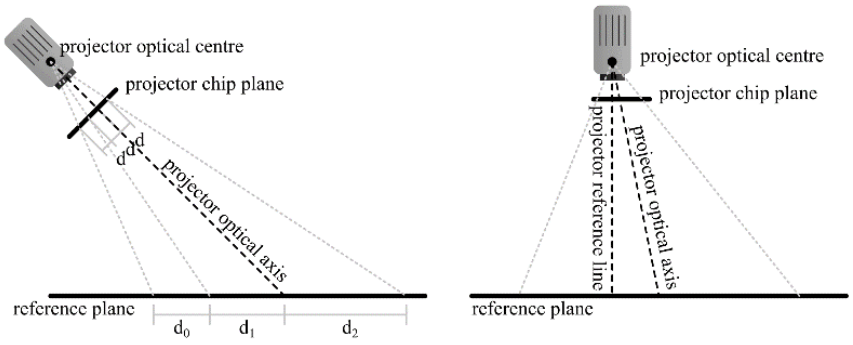

(a) (b)

Figure 2: Light propagation path of projector: (a) when positioned at an acute angle to orthogonal of reference plane, and (b) when positioned orthogonally to reference plane.

2 PRINCIPLE

In the proposed model, both the camera optical axis and projector reference line is placed orthogonal to the reference plane as shown in Figure 3. Three conditions must be met for this model to function appropriately, including (1) the camera optical axis and projector reference line must be orthogonal to the reference plane, (2) the object to be measured must be within the overlapped light path area between the camera and the projector (triangle ABC shown in Figure 3), and (3) the end of the image acquisition area, point *C*, needs to be placed before the projector reference line. In relation to condition (1), the proposed model simplifies the triangulation trigonometric relationship and reduces the number of model parameters to three, i.e. h_c (camera optical centre height), h_p (projector optical centre height) and q (distance between camera optical axis and projector optical axis). Meanwhile, condition (2) ensures that the object surface is projected with the fringe image and within region of image acquisition of the camera. To convert the phases into height, areas from point *A* to point *O*, point *O* to projector reference line and area to the right of projector reference line in Figure 3, three different mathematical equations would be required. The area of projection to the right of projector reference line is too small for measuring object while also requiring an additional mathematical equation. Condition (3) limits the area of image acquisition from point *A* to point *O* and from point *O* to point *C*. By limiting the area of image acquisition within segment *AC*, the complexity of the phase to height conversion would also be reduced.

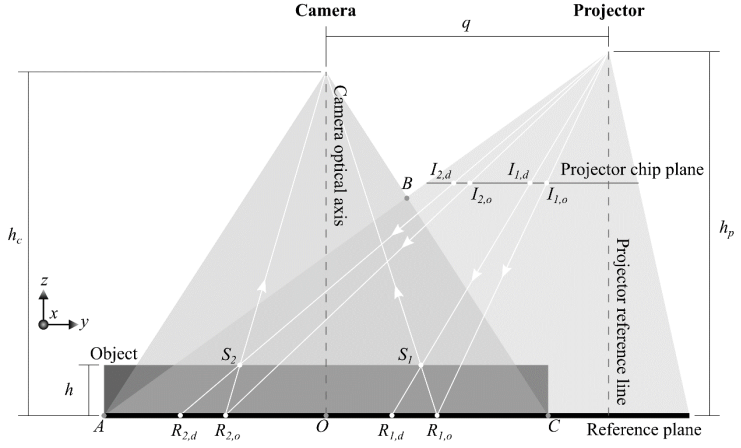

Figure 3: Configuration layout of the proposed model.

In order to derive the equations for phase to height conversion, the affiliated model parameters, i.e. h_c, h_p and q, must be determined first. A cuboid object with known height, h_o was placed under the profilometry system as shown in Figure 4. A line profile was projected onto the reference plane and the object surface. The distance between the line profile and image centre were computed from the *y*-coordinate of the line profile in the respective acquired images. These distances, i.e. distance on reference plane and distance on object surface were labelled v_1 and v_2 respectively as shown in Figure 4 (a). The camera optical centre height with respect to the reference plane, h_c, would be calculated by applying the following equation:

$$h_c = \frac{v_2}{v_2 - v_1} \cdot h_o \quad (1)$$

For h_p and q, two line profiles were projected onto the reference plane and the object surface. The distance between the line profiles and the image centre were computed from the y-coordinate of the line profile in the respective acquired images. These distances, i.e. distances on reference plane and distances on object surface, were labelled as φ_1, φ_2, γ_1 and γ_2, respectively, as shown in Figure 4 (a). By relating h_o and h_p to α_1 and α_2, the following relationships can be formed:

$$\tan\alpha_1 = \frac{h_o}{\varphi_1 - \gamma_1} = \frac{h_p}{\varphi_1 + q} \quad (2)$$

$$\tan\alpha_2 = \frac{h_o}{\varphi_2 - \gamma_2} = \frac{h_p}{\varphi_2 + q} \quad (3)$$

The projector optical centre height with respect to the reference plane, h_p and the distance between camera optical axis and projector optical axis, q can be calculated by solving both Eq. (2) and Eq. (3) simultaneously as follows:

$$q = \frac{\varphi_2\gamma_1 - \varphi_1\gamma_2}{(\varphi_1 - \varphi_2) - (\gamma_1 - \gamma_2)} \quad (4)$$

$$h_p = h_o \cdot \frac{\varphi_1 + q}{\varphi_1 - \gamma_1} \quad (5)$$

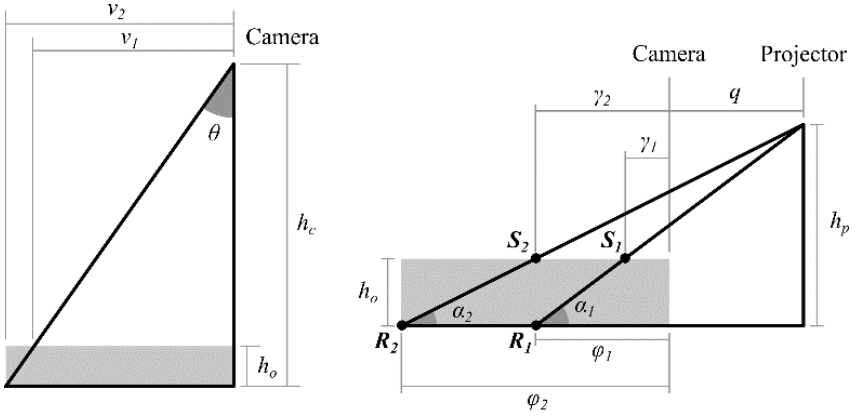

(a) (b)

Figure 4: Light path diagrams from Figure 3: (a) for determining h_c, and (b) for determining h_p and q.

The phase to height conversion was separated into two segments, namely the *OC* and *AO* as shown in Figure 5 (a) and Figure 5 (b), respectively. For points located between *OC*, such as S_1, the height and y-coordinate can be related to angle α and β, as follows:

$$\tan\alpha = \frac{h}{y_1 - b} = \frac{h_p}{q - b} \quad (6)$$

$$\tan\beta = \frac{h}{a - y_1} = \frac{h_c}{a} \quad (7)$$

By solving Eq. (6) and Eq. (7) simultaneously, the height and y-coordinate of S_1 can be determined using the following expressions:

$$h = h_c\left(1 - \frac{y_1}{a}\right) \quad (8)$$

$$y_1 = \frac{h_c(q-b) + h_p b}{h_c\left(\frac{q-b}{a}\right) + h_p} \quad (9)$$

where a is the phase on the reference plane and b is the phase on the object surface. For points located between *AO*, such as S_2, the height and y-coordinate could be related to angle α and β, as follows:

$$\tan\alpha = \frac{h}{b - y_2} = \frac{h_p}{b + q} \quad (10)$$

$$\tan\beta = \frac{h}{a - y_2} = \frac{h_c}{a} \quad (11)$$

By solving Eq. (10) and Eq. (11) simultaneously, the height and y-coordinate of S_2 can be determined by applying the following expressions:

$$h = h_c\left(1 - \frac{y_2}{a}\right) \quad (12)$$

$$y_2 = \frac{h_c(q+b) - h_p b}{h_c\left(\frac{q+b}{a}\right) - h_p} \quad (13)$$

The x-coordinate for both points S_1 and S_2 could be calculated by employing the following trigonometry-based expressions (as shown Figure 5 (c)):

$$\tan\alpha = \frac{h}{x_R - x_O} = \frac{h_c}{x_R} \quad (14)$$

$$x_O = x_R\left(1 - \frac{h}{h_c}\right) \quad (15)$$

where x_R is the x-coordinate on reference plane.

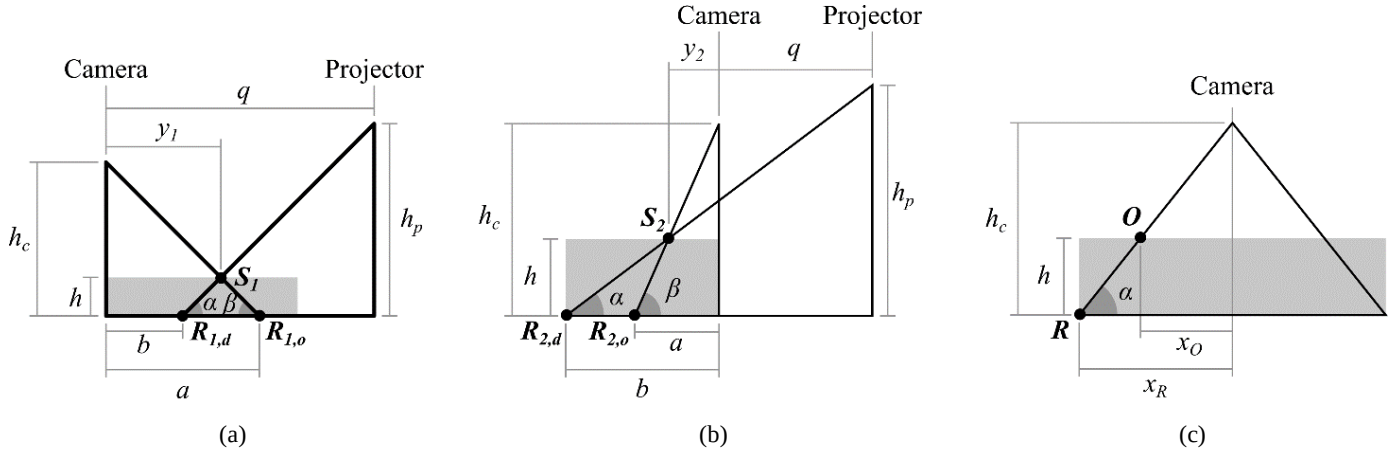

Figure 5: Light path diagrams from Figure 3: (a) for determining *y* and *h* at point S_1, (b) for determining *y* and *h* at point S_2, and (c) for determining *x* at point *R*.

3 EXPERIMENT AND VERIFICATION

A profilometry system was set up based on the proposed model. The system comprised of an Epson EBX04 LCD Projector, a Basler ace acA2500-14uc colour CCD camera and a processing unit (Dell Inspiron 14R SE 7420 with Intel i7-3612QM CPU@2.10 GHz and 8 GB RAM). De Bruijn's colour-coded fringe pattern was used as the projection pattern. The phase demodulation and phase unwrapping processes were based on a single frame profilometry system described in our previous work [7]. The algorithms were written in MATLAB 2017b. A cuboid, a triangular beam and a fan blade (as shown in Figure 6) were reconstructed using the profilometry system as shown in Figure 7. The cross-section profiles of the objects were compared to the actual dimensions. The reference fan blade surface was reconstructed from a point cloud of 164 coordinates using Mitutoyo CRYSTA-Plus M Series 196 coordinate measuring machine (CMM). Point *O* in Figure 6 (c) was the mean coordinate for point *A* to point *H* on the fan blade. All the cross-sectional profiles were centred at the intersection of each cross-section lines and the lines passed through point *O* and normal to the cross section lines. The reconstructed cross section profiles and their *z*-axis error were depicted in Figure 8. The confidence interval (CI) at 95% confidence level (CL), root mean square (RMS) and standard deviation (SD) for *z*-axis error at sections *AA'*, *BB'*, *AE*, *BF*, *CG* and *DH* were tabulated in Table 2.

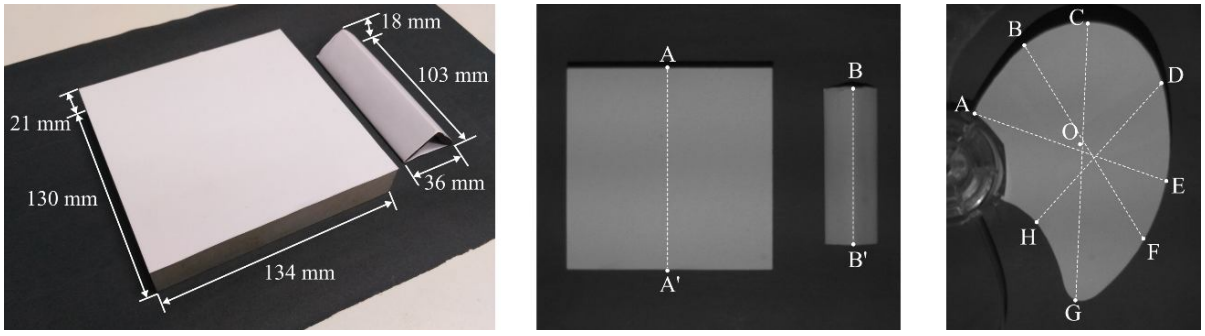

Figure 6: Objects for model verification: (a) cuboid and triangular beam, (b) cross section lines of cuboid and triangular beam, and (c) fan blade with cross section lines and centroid.

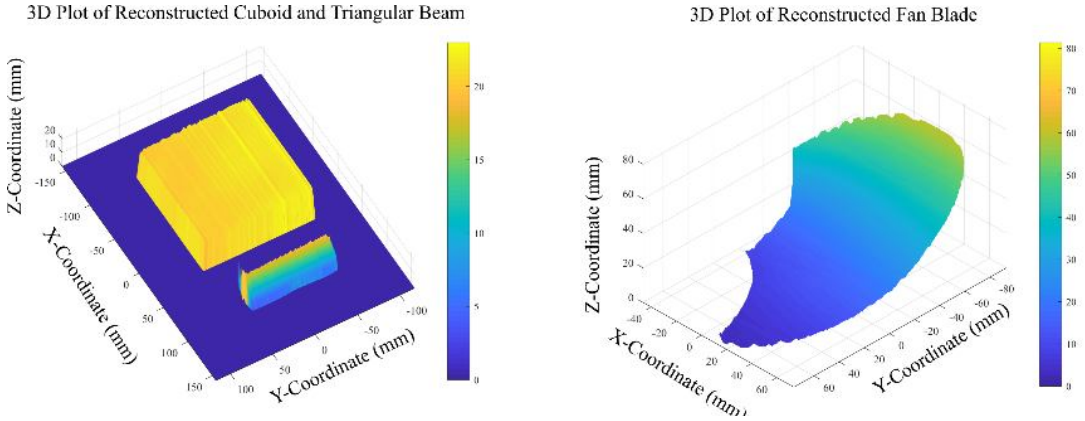

(a) (b)

Figure 7: Reconstructed objects: (a) cuboid and triangular beam, and (b) fan blade.

Table 2: Error parameters for all cross-section profiles.

Object	Section	CI at 95% CL (mm)
Cuboid	*AA'*	(0.07 ± 0.04)
Triangulation	*BB'*	(0.10 ± 0.04)
Fan blade	*AE*	(2.61 ± 0.20)
	BF	(2.61 ± 0.20)
	CG	(2.70 ± 0.20)
	DH	(2.61 ± 0.20)

4 RESULT AND DISCUSSION

Figure 8 and Table 2 reflects the result of the reconstruction based on the proposed model. The cross-section profile errors, as depicted in Figure 8, were determined by comparing the reconstruction profile to the fitted reference value obtained by CMM. The shape of the reconstructed profiles generally resembled the actual objects as observed in Figure 8. Wavy artefacts were seen on the reconstructed surfaces in Figure 7 and Figure 8. These artefacts were attributed to a phenomenon known as gamma non-linearity. It occurred due to a phase error caused by the non-linearity of the projection output and deviation of light intensity levels from the expected sinusoidal pattern[8-11].

As reflected in Table 2, the errors (at 95% confidence level) for cuboid and triangular beam were recorded at 0.07 ± 0.04 mm and 0.10 ± 0.04 mm respectively. On the curved surface, the average errors, at 95% confidence level, for sections *AE*, *BF*, *CG* and *DH* were recorded at 2.63 ± 0.20 mm. The differences of the errors between flat and curved surface were due to the changes in the surface height gradient. Changes in the surface height gradient affected brightness of the fringe pattern that the camera acquired as the light was deflected away from the camera sensor plane. This caused the acquired intensity profile to be inaccurate resulting in the margin of errors for a curved surface to be larger than that of a flat surface. This was reflected in the means of errors where the largest errors were found in the curved surface such as sections *AE*, *BF*, *CG* and *DH*, followed by slanted surface such as section *BB'* of triangular beam and lastly, section *AA'* of the cuboid.

The uncertainty of the errors in sections *AA'* and *BB'* were small since the cross-section profiles were flat. The large changes in the surface height gradient in the fan blade also increased the margin of errors since the range focal plane of the camera and projector could be smaller than the range of object height. These factors increased the bias and gamma errors which resulted in the sharp increases in the mean and confidence interval for errors in sections *AE*, *BF*, *CG* and *DH* in comparison with sections *AA'* and *BB'*. However, the uncertainty of the errors consistently fluctuated within ± 0.20 mm (at 95% confidence level) indicating the accuracy of the proposed method. By considering the actual profile of the curved surface (section *CG*) which spanned for 57.98 mm, the uncertainty of the measurement would be 0.34%. The results of the proposed model were comparable to the reported works while using less model parameters and simpler calibration process with any generic projector.

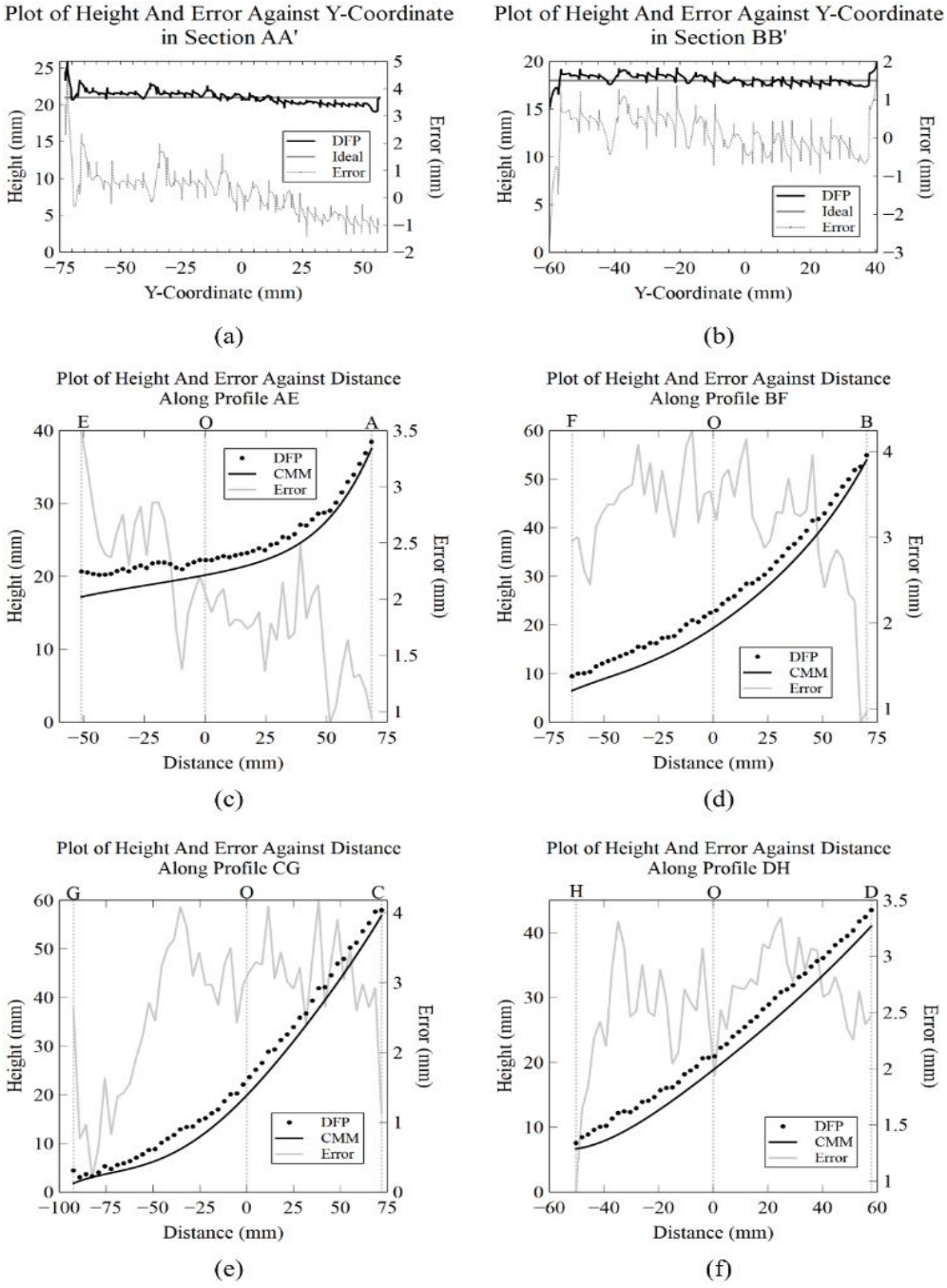

Figure 8: Cross section profiles and errors: (a) section AA' in cuboid, (b) section BB' in triangular beam, (c) section AE in fan blade, (d) section BF in fan blade, (e) section CG in fan blade, and (f) section DH in fan blade.

In order to increase accuracy of the profilometry system, a compensation algorithm could be employed to remove the bias error. Small angle changes in optical axis and the resolution for the projector and camera also affect the accuracy of the distances measured when calculating h_c, h_p and q. This issue may be alleviated by adopting a more appropriate calibration technique and high accuracy angle measuring equipment. Using gamma correction algorithm and better equipment, such as camera and projector with higher resolution, contrast and brightness specifications, could also facilitate reduced gamma error. Therefore, enabling smaller error confidence interval and improved consistency.

5 CONCLUSION

This research has proposed a simplified geometric model for generic application in digital fringe profilometry. The proposed model enables a simpler calibration process pre-measurement by (1) determining only three parameters, (2) eliminating inconsistency of fringe width, and (3) applying more suitable light path configuration for the projector. Experimental result shows that the model is capable of reconstructing the object

surface consistently. The errors were recorded at 0.07 ± 0.04 mm (over 21 mm height), 0.10 ± 0.04 mm (over 18 mm height) and 2.63 ± 0.20 mm (over 57.98 mm height) for flat, slanted and curved surfaces, respectively. The results of the proposed model are comparable to the results of other reported works. Direct compensation algorithm could be applied in addressing bias errors to increase measurement accuracy without upgrading the hardware. Solving gamma non-linearity could further improve both the accuracy and consistency of the system. Additionally, more appropriate calibration technique is an alternative to the model accuracy improvement and could potentially be further studied in future work.

ACKNOWLEDGEMENT

This research was supported by the Universiti Sains Malaysia Bridging Grant (Grant no. 304.PMEKANIK.6316123). The authors would like to acknowledge the generosity of Numeral Engineering Sdn. Bhd. in providing the fabrication service for this research.

REFERENCES

[1] Gorthi SS, Rastogi P, "Fringe projection techniques: Whither we are?" *Optics and Lasers in Engineering, 48*(2), 133-140, doi:10.1016/j.optlaseng.2009.09.001, 2010.

[2] Zappa E, BuscaG, "Static and dynamic features of Fourier transform profilometry: A review." *Optics and Lasers in Engineering, 50*(8), 1140-1151, doi:10.1016/j.optlaseng.2012.03.008, 2012.

[3] Huang Z, Xi J, Yu Y, Guo Q, Song L, "Improved geometrical model of fringe projection profilometry." *Optics Express, 22*(26), 32220-32232, doi:10.1364/OE.22.032220, 2014.

[4] Takeda M, Mutoh K,"Fourier transform profilometry for the automatic measurement of 3-D object shapes." *Applied Optics, 22*(24), 3977-3982, doi:10.1364/ao.22.003977, 1983

[5] Mao X, Chen W, Su X, "Improved Fourier-transform profilometry." *Applied Optics, 46*(5), 664-668, doi:10.1364/ao.46.000664, 2007.

[6] Xiao Y, Cao Y, Wu Y, "Improved algorithm for phase-to-height mapping in phase measuring profilometry. *Appl Opt, 51*(8), 1149-1155, doi:10.1364/AO.51.001149, 2012.

[7] Yee CK, Yen KS, "Single frame profilometry with rapid phase demodulation on colour-coded fringes." *Optics Communications, 397*, 44-50, doi:10.1016/j.optcom.2017.03.064, 2017.

[8] Cui H, Zhao Z, Wu Y, Dai N, Cheng X, Zhang L, "Digital fringe image gamma modeling and new algorithm for phase error compensation." *Optik - International Journal for Light and Electron Optics, 125*(24), 7175-7181, doi:10.1016/j.ijleo.2014.07.109, 2014.

[9] Guo H, He H, Chen M, "Gamma correction for digital fringe projection profilometry." *Applied Optics, 43*(14), 2906-2914, doi:10.1364/ao.43.002906, 2004.

[10] Hoang T, Pan B, Nguyen D, Wang Z, "Generic gamma correction for accuracy enhancement in fringe-projection profilometry." *Optics Letters, 35*(12), 1992-1994, doi:10.1364/OL.35.001992, 2010.

[11] Li Z, Li Y, "Gamma-distorted fringe image modeling and accurate gamma correction for fast phase measuring profilometry." *Optics Letters, 36*(2), 154-156, doi:10.1364/OL.36.000154, 2011.